

Multibody Dynamics Simulation of Planar Linkages with Dahl Friction

E. Pennestrì, P.P. Valentini, L. Vita

Dip. Ingegneria Meccanica, Università di Roma Tor Vergata, 00133 Roma - Italy

Abstract

It is well known that classical Coulomb dry friction model does not portrays important physical phenomena occurring in the contact between mating surfaces. Moreover, the discontinuity of force at zero velocity has many drawbacks during numerical simulations. In the attempt of exploring alternatives to Coulomb friction model, this paper present the application of the Dahl friction model in a multibody dynamics formulation. The analysis herein presented includes also the modeling of friction forces in lower pairs and some hints on the efficient computation of Lagrange parameters during the fixed-point iteration process. Two numerical examples are offered.

Keywords: Friction, Dahl friction model, planar linkages

Nomenclature

Unless otherwise stated in the text, the following nomenclature is used:

- $[A_i]$: transform matrix from $G_i - x_i y_i$ to $O - XY$;
- $[B_i]$: $\frac{d[A_i]}{dq_{3i}}$
- $[C_{i_k}]$: transform matrix from $P_k - x_{i_k} y_{i_k}$ to $G_i - x_i y_i$;
- F_a : friction force according to Dahl model;
- F_c : Coulomb friction force which is obtained multiplying friction coefficient μ_d by the force N normal to the surface;
- g : gravity acceleration;
- $G_i - x_i y_i$ body fixed Cartesian system of axes with origin in the center of mass of the i^{th} body;
- J : number of kinematic pairs;
- L : slider length;
- m_i : mass of the i^{th} particle;
- $[M]$: the mass matrix;
- $O - XY$ inertial Cartesian system of axes;
- $\{q\}$: generalized coordinates vector;
- $\{ q_{3i-2} \quad q_{3i-1} \}$: Absolute coordinates of center of mass of the i^{th} body;

- q_{3i} : Angular position of the i^{th} body;
- $\{Q_{a_k}^{(i)}\} \equiv \{ F_{a_x} \ F_{a_y} \ T_z \}^T$ generalized friction force acting on the body i^{th} through the k^{th} kinematic element;
- $\{Q_a\}$: Generalized vector of friction forces;
- r_k radius of the bearing;
- x_r : relative tangential displacement between mating kinematic elements;
- t : time;
- T : period of free mass oscillation in the absence of friction;
- v_r : \dot{x}_r ;
- z : elastic displacement between contacting surfaces;
- $\{\gamma\} = -([\Psi_q] \{\dot{q}\})_q \{\dot{q}\}$
- $\{\lambda\}$: the vector of Lagrange multipliers;
- μ_s, μ_d : static and dynamic Coulomb friction coefficients, respectively;
- $[\Psi_q]$: the Jacobian matrix of the kinematic scleronomic and rheonomic constraints
- σ : coefficient of contact stiffness of the Dahl friction model;
- $P_k - x_{i_k} y_{i_k}$ the joint Cartesian system of axes associated with the k^{th} kinematic element of the i^{th} body;
- $\text{chol}(\cdot)$ Upper triangular matrix resulting from Cholesky factorization;
- $\text{sgn}(v_r) = +1$ if $v_r > 0$, $\text{sgn}(v_r) = -1$ if $v_r < 0$;
- The superscript $+$ denotes the pseudo inverse of a matrix.
- Dots denote differentiation with respect to time.

1 Introduction

Friction is a very important factor in mechanical systems. Because of its importance one should take it into account at the early stages of engineering design. In order to reduce the differences between numerical simulation and experimental results, friction models should be embedded in multibody dynamics equations.

The availability of sophisticated measurement techniques and the great practical importance of the topic stimulated experimental tests for the analysis of elastic and plastic deformation forces between the surfaces asperities in contact. Devised in 1785, the Coulomb dry friction model portrays kinetic friction in a satisfactory manner for engineering purposes. The transition from static to kinetic is instead handled by means of a physically unrealistic instantaneous change of force. Obviously the inadequacy of testing equipment at Coulomb's times did not allowed the distinguished French scientist to give a more detailed account of the friction phenomena. It should be observed that the simplicity of the Coulomb dry friction model is only apparent. In fact, there are several numerical challenges in the numerical simulation of systems with embedded such a model. The situation is very well depicted by the following statement of C. Glocker [1]

With that friction law, one has chosen one of the most complicated force laws that occur in application problems. It seems so easy and so clear at first view, however, when trying to apply it, or even just trying to write it down a mathematical expression, one immediately encounters a lot of serious and not expected problems of different nature.

Regardless of this, there is a vast amount of literature dealing with the development of models embedding Coulomb friction. For instance, thoughtful contributions to the problem of impact in multibody systems in the presence of Coulomb dry friction are due to F. Pfeiffer, C. Glocker [2], Y. Wang, Mason [3], S. Ahmed, I. Han, B.J. Gilmore [4], H.M. Lankarani and M.F.O.S. Pereira [5], H.M. Lankarani [6], W.J. Stronge [7], D. Centea, H. Rahnejat, M.T. Munday [8].

Experiments evidenced many complex friction phenomena not covered by the dry friction model. However, despite the effort of many researchers, friction physical mechanisms still elude a complete and comprehensive quantification. Broadly speaking two different friction states can be observed: the *sticking* and the *sliding* phase. During the sticking phase, when relative motion between contacting surfaces is absent or observed at microscopic level only, friction force is predominately a function of displacement. During the *sliding* phase velocity may have a not negligible influence, as observed for instance in the Stribeck effect.

The growth of precision applications and the need of reliable control schemes brought to the development of innovative analytical friction models and parameter identification procedures [9, 10, 13, 12, 14, 15]. The challenge was the casting of a friction model with the following features:

- reasonable mathematical complexity;
- capability to capture the essence of the complicated friction phenomena.

In 1968 P.R. Dahl [9] proposed an innovative friction model. This was based on the experimental evidence that small amplitude friction forces were reacted against by small elastic restoring forces. From this observation, a solid friction model was developed. The Dahl *dynamic friction model* was later improved by H. Olsson *et al.* to include the Stribeck effect [13].

The authors of this paper investigated the possibility of embedding the Dahl friction model into a multibody dynamics formulation. Although there is not a general consensus on the *best* dynamic friction model, a comparative investigation observed that the Dahl model provides a reliable representation of friction behavior near zero velocity [12].

The purpose of this paper is to discuss also the difficulties involved in the simulation of planar linkages with friction and to test the introduction of the Dahl friction model in a multibody dynamics code. The main reasons for adopting such a model are:

- the accuracy of the model has been confirmed by experimental tests in many practical cases;
- avoidance of the mathematical discontinuity at zero velocity.

In our analysis we admit rigid body motion, absence of impacts and clearances in kinematic pairs.

This paper is organized in four parts. In the first part the classical dry Coulomb model is discussed, some of the difficulties involved are mentioned and previous contributions of analysis of planar linkages with friction reviewed. The second part focuses on internal states friction modeling with particular attention to the Dahl model. The

third part presents the proposed dynamic formulation and the modeling of friction in revolute and prismatic pairs. In particular, the modeling of friction in revolute joints has been refined with respect to the one presented in [35]. Moreover, it has been shown that the computation of Lagrange multipliers during fixed-point iteration does not involve the computation of generalized accelerations. Finally, the fourth part includes numerical examples and conclusions.

2 The dry friction Coulomb model and inherent difficulties

In linkages with one or two degrees-of-freedom, the friction in revolute pairs should not alter the direction of reactions in a sensitive manner. Thus, under such circumstances, engineering analysis usually ignores friction. This assumption is unjustified if a small change of configuration produces large changes in the magnitude of related forces. This situation, common for instance in mechanical presses, happens in mechanisms whose configuration is close to singularity.

The Coulomb dry friction model is widespread in the modeling of mechanical systems. Although has been critically reviewed by many researchers, it is still widely applied and considered reliable in many instances.

The Coulomb dry friction model of prismatic and revolute pairs is often discussed at basic textbook level.

The usual scheme used to introduce the Coulomb empirical law is shown in Figure 2 and refers to a one degree-of-freedom mechanical system.

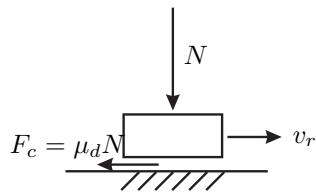


Figure 1: The introductory example of Coulomb dry friction model

Coulomb law states that friction force F_c is bounded in magnitude by the product of the reaction force normal component (N) times the friction coefficient (μ_d).

If $v_r = 0$ then $F_c \leq \mu_s |N|$. Otherwise, if $v_r \neq 0$, then $F_c = -\mu_d |N| \operatorname{sgn}(v_r)$.

It is evident that differential equations of models with Coulomb friction contain discontinuities of the state variable v_r which complicate their solution.

Despite its apparent simplicity, there are different numerical problems which plague the simulation of mechanical systems subjected to Coulomb friction.

Non-uniqueness and non existence of solution for accelerations.

The first monograph pointing out such problems has been authored in 1895 by P. Painlevé [18]. In the preface it is stated:

La connaissance de la loi de frottement du système \mathcal{S} et des forces actives permet de calculer le mouvement de \mathcal{S} , mais laisse parfois le choix entre plusieurs mouvements possibles répondant aux mêmes conditions initiales.

An example of such non-uniqueness of solution has been provided by P. Painlevé (see [18] p.93) and further thoughtfully discussed by H.J. Klepp [19, 20] and P. Dupont [21].

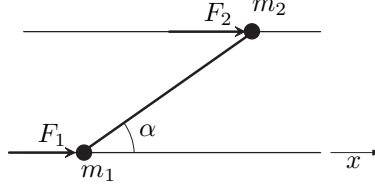


Figure 2: Example proposed by Painlevé to discuss non uniqueness

With reference to Figure 2 let us consider the point masses m_1 and m_2 sliding along two horizontal parallel lines. The masses are connected with a massless rigid bar forming the constant angle α with the horizontal line. Let F_1 and F_2 be the horizontal forces acting on the masses m_1 and m_2 , respectively and μ_{d1} and μ_{d2} the friction coefficients between the masses and the lines.

Assuming, $m_1 = m_2 = 1$, $F_1 > F_2$, $0 < \alpha < \frac{\pi}{2}$, $\mu_{d1} > \mu_{d2}$, the dynamic equilibrium equations for the two masses are

$$\ddot{x}_1 = F_1 - R \cos \alpha - \varepsilon \mu_{d1} R \sin \alpha , \quad (1a)$$

$$\ddot{x}_2 = F_2 + R \cos \alpha - \varepsilon \mu_{d2} R \sin \alpha , \quad (1b)$$

where R is the force along the connecting bar and

$$\varepsilon = \begin{cases} +1 , & \text{when } R\dot{x} > 0 \\ -1 , & \text{when } R\dot{x} < 0 \end{cases} \quad (2)$$

Because of connecting bar rigidity $\ddot{x}_1 = \ddot{x}_2$, therefore from the previous equations, one obtains

$$R = \frac{F_1 - F_2}{2 \cos \alpha + \varepsilon (\mu_{d1} - \mu_{d2}) \sin \alpha} . \quad (3)$$

When

$$2 \cos \alpha < (\mu_{d1} - \mu_{d2}) \sin \alpha \quad (4)$$

and the algebraic signs of $(F_1 - F_2)$ and \dot{x} are the same, the equations of motion (1) give the choice of two possible motions.

Another classical example, used to elucidate an apparent inconsistency associated with Coulomb friction law and rigid body motion, has been also discussed by Painlevé in a series of papers [18, 22].

With reference to Figure 3, a disc of mass M , radius r , radius of giration k , angular velocity ω is sliding with velocity v_r on a planar surface. The center of mass G does not coincide with the center C of the disc. The bodies in contact are rigid and the disc always maintains contact with the surface. Rolling friction is neglected.

From the dynamic equilibrium conditions one obtains

$$M\ddot{X}_G = F_c , \quad (5a)$$

$$M\ddot{Y}_G = N - Mg , \quad (5b)$$

$$Mk^2\dot{\omega} = F_cb - Na . \quad (5c)$$

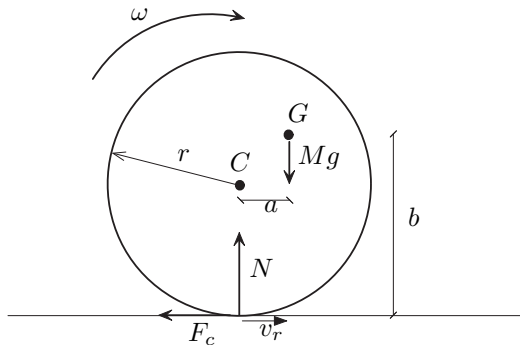


Figure 3: Example proposed by P. Painlevé (1905) to discuss the homonym paradox [22]

For $\ddot{Y}_C = 0$, then $\ddot{Y}_G = a\dot{\omega} - (b-r)\omega^2$, and from (5) the following equality can be established¹

$$M[(r-b)\omega^2 + g]k^2 = N(a^2 + k^2) - F_c ab. \quad (6)$$

When $[(r-b)\omega^2 + g] > 0$, assuming $a > 0$, $b > 0$, $N > 0$, $F_c > 0$, then from (6) follows

$$\frac{F_c}{N} < \frac{k^2 + a^2}{ab}. \quad (7)$$

This inequality is not consistent with the value of μ_d required by the Coulomb law. Apparently Coulomb law is not consistent with rigid body dynamics. However, as remarked by D.E. Stewart [23], this line of reasoning is flawed by the assumption that all forces are bounded functions of time. In fact, one should not rule out the possibility that the velocity \dot{X}_C could be brought to zero instantaneously by impulsive contact forces. In such a case no longer holds the Coulomb equality $F_c = \mu_d N$.

Friction force discontinuity is a challenge for the numerical integration procedure.

The sudden change of force associated with the change of velocity sign causes the numerical integration algorithm to reduce the size of the step. This obviously increases computation time and accuracy. In the attempt to diminish the sensitivity to the discontinuity, numerical algorithms of low-order and low-accuracy are sometime used [24]. Alternatively, smooth nonlinear friction law instead of the Coulomb's friction law can be used. For instance, the following law is often adopted [9, 14, 25]

$$F_a = -\mu \tanh\left(\frac{v_r}{\gamma}\right) N \quad (8)$$

where γ is a limit speed at which microsliding occurs. This approach has the adverse effect of making stiff the ODEs system [14]. Thus a trade-off must be chosen to select the appropriate value of γ . Another drawback is that at zero relative velocity the computed friction force is also equal to zero.

A review of alternative continuous friction force laws is presented by B. Armstrong-Helouvry [10]

An interesting approach to numerical integration of differential equations with discontinuities is due to A.F. Filippov (see [36], p.213 for an application of such approach).

¹The minus sign before F is due to the orientation of v_r assumed in Figure 3.

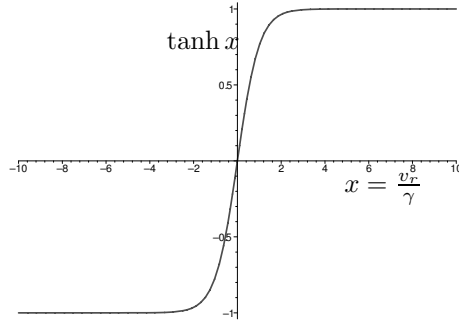


Figure 4: Smooth friction law

Let us assume that the following differential equation must be solved

$$\ddot{q} = f(t, q, \dot{q}) = \begin{cases} f^+ & \text{for } v_r > 0 \\ f^- & \text{for } v_r < 0 \end{cases} \quad (9)$$

When the condition

$$v_r(t, q, \dot{q}) = 0 \quad (10)$$

is fulfilled, Filippov introduced a new solution of the differential equation by allowing the right-hand side term to be a linear combination of its extreme values

$$\ddot{q} = \varepsilon f^+ + (1 - \varepsilon) f^- , \varepsilon \in [0, 1] . \quad (11)$$

Combining (10) and (11) one obtains a differential-algebraic equations (DAE) system to be solved for q , \dot{q} and ε .

In particular, introduced the directional derivatives of the switching functions

$$Dv_r^+ := \frac{\partial v_r}{\partial t} + \frac{\partial v_r}{\partial q} \dot{q} + \frac{\partial v_r}{\partial \dot{q}} f^+ , \quad (12)$$

$$Dv_r^- := \frac{\partial v_r}{\partial t} + \frac{\partial v_r}{\partial q} \dot{q} + \frac{\partial v_r}{\partial \dot{q}} f^- , \quad (13)$$

if $v_r = 0$ and provided that such directional derivatives have opposite algebraic sign, then [36]

$$\ddot{q} = \frac{Dv_r^+ f^- - Dv_r^- f^+}{Dv_r^+ - Dv_r^-} \quad (14)$$

and

$$\varepsilon = - \frac{Dv_r^-}{Dv_r^+ - Dv_r^-} . \quad (15)$$

In kinematic pairs with no relative motion the computation of friction forces is not straightforward.

An updated list of references on the influence of friction on mechanical systems has been compiled by R.A. Ibrahim [26] and B. Armstrong-Hélouvry, P. Dupont, C. Canudas [27].

Most of the previous comments on the difficulties of simulating mechanical systems subjected to Coulomb friction are very well condensed by the statement made J. de Jalón and E. Bayo in their textbook [28]:

The mathematical model for the Coulomb friction is not easy to implement in general purpose codes, even for the simplest cases. It is not currently implemented with generality in any commercial simulation package to the authors' knowledge. The difficulties stem from the switching between sliding and stiction states involving a change in the number of the system degrees of freedom and the need to iterate, in the sliding state, for each acceleration evaluation.

Another excellent example of the numerical difficulties associated with the simulation of systems composed of masses subjected to classical Coulomb dry friction model is provided by Pfeiffer and Glocker [2] (see p. 7).

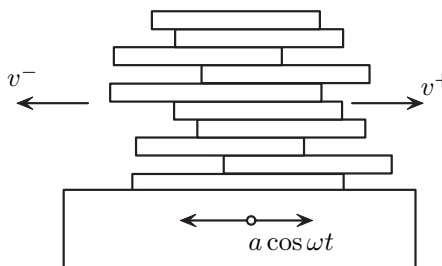


Figure 5: Combinatorial problem associated with motion simulation of sliding masses subjected to Coulomb friction (adapted from [2])

With reference to Figure 5, let us consider ten masses collected into a pile with sliding contacts and subjected to gravity. There are three possibilities for the motion of each mass: move to the left with v^- velocity, move to the right with v^+ velocity, or not move at all. This results into $3^{10} = 59,049$ possibilities of combinations of constraints to be tested at each integration step. The task associated with the combinatorial problem is usually simplified by introducing the concept of complementarity behavior of unilateral contacts (*e.g.* [1, 2]).

3 The Dahl dynamic friction model

The Dahl model [9, 10, 11, 12, 13] is based on the observations made during experimental analyses on systems with ball bearings. He noted that, within a certain limit, input forces were reacted by elastic restoring forces. These are due to the quantum mechanical bonds between the surfaces in contact. These bonds break once the input force exceeds a given limit. This behavior is somewhat similar to the one observed in material deformation tests. Hence Dahl developed his continuous friction force-displacement relationship on the base of the analogy with stress-strain behavior. Continuing with this analogy, for Dahl the transition from static to kinetic friction corresponds to the transition from elastic to plastic deformation in ductile materials. Hence, for low tensile loads, a spring-like behavior is observed. After the relaxation of the load the system returns into the original unstressed state. When the load is larger the bonds break and the system will not return to its original state and an hysteresis appears.

The bristle model, depicted in Figure 6, is commonly used to convey the reasoning behind the described behavior.

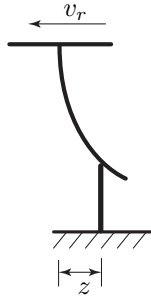


Figure 6: The bristle analogy for Dahl model.

Up to a certain applied load, the intersection point of the bristle neither changes nor moves. The elastically deformed bristles return to their original state after the load removal. The stiffness σ of the bristle characterizes the elasticity of the contact surfaces. Once exceeded the elastic resistance, the entire brush moves and a permanent displacement occurs. The Dahl model introduces a lag in the a Coulomb friction model when relative velocity reverses sign.

Let x_r and v_r be respectively the relative tangential displacement and relative velocity between the mating surfaces of the generic k^{th} kinematic pair². According to Dahl the actual friction force F_a and the Coulomb friction force F_c are related by the differential equation

$$\frac{dF_a}{dx_r} = \sigma \left(1 - \frac{F_a}{F_c} \text{sign}(v_r) \right)^\alpha \quad (16)$$

where

- σ is the contact stiffness coefficient, it can be interpreted as the slope of force-displacement curve at $F = 0$;
- α is a parameter influencing the shape of the $F_a(x)$ curve.

Since $dx_r = v_r dt$, according to [16], the Dahl model is also expressed by the following differential equation

$$\frac{dF_a}{dt} = \sigma v_r \left| 1 - \frac{F_a}{F_c} \text{sign}(v_r) \right|^\alpha \text{sgn} \left(1 - \frac{F_a}{F_c} \text{sign}(v_r) \right) . \quad (17)$$

As shown in Figure 7, the parameter α determines the shape of the input force-output displacement hysteresis maps of the Dahl model³. This parameter was used by Dahl for matching experimental results. The empirical values of $\alpha = 1$ and $\alpha = 1.5$ are usually hinted [12]. For $\alpha \geq 1$ the right-hand side of (17) is Lipschitz continuous [16]. In the theory of differential equations, Lipschitz continuity is the central condition of the Picard-Lindelöf theorem [17] which guarantees the existence and uniqueness of the solution to an initial value problem.

Alternatively, according to [15], after we let

$$F_a = \sigma z , \quad (18)$$

²The subscript k in the formulas of this section is omitted for simplicity.

³The plots have been generated with the following data $F_c = 0.75$, $\sigma = 15$, $x_r = 0.1 \sin 0.1t$.

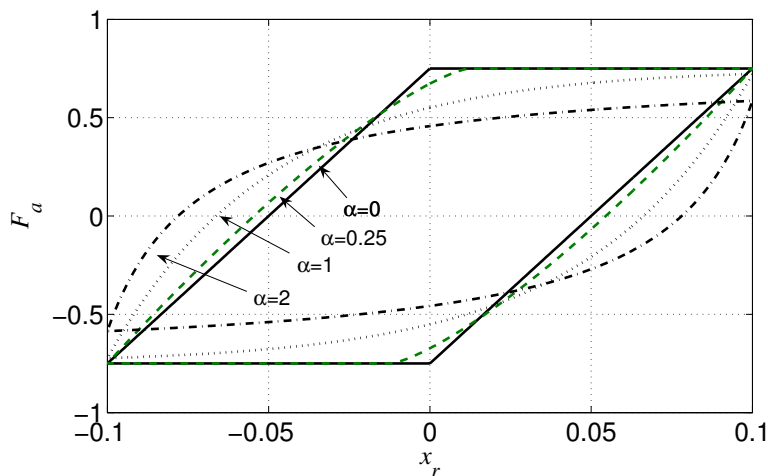


Figure 7: Dahl model: Influence of α on the force-displacement curve.

equation (16) can be rewritten in the form

$$\frac{dz}{dt} = v_r \left(1 - \frac{\sigma z}{F_c} \text{sign}(v_r) \right)^\alpha . \quad (19)$$

There are several bibliographical references (*e.g.* [43, 44]) where procedures for the identification of friction parameters α and σ are discussed and applied to practical cases.

The use of dynamic friction models in multibody dynamics code has been discussed by M. Morandini (see [29], p.496-498).

4 Force analysis of linkages with Coulomb friction - Review of previous contributions

This section mainly reviews analyses of planar linkages and mechanisms in the presence of Coulomb friction. Our review will be focused mainly on treatments reported in textbooks.

One of the first textbooks entirely dedicated to the analysis of linkages with Coulomb friction has been authored by G. Herrmann [30]. His graphical method of analysis considers systems with both revolute and prismatic pairs. Mechanical efficiency analyses of simple levers and simple linkages are executed under the hypotheses of impending motion and static working conditions (See Figure 8 for a sample of the graphical constructions required by the method of Herrmann).

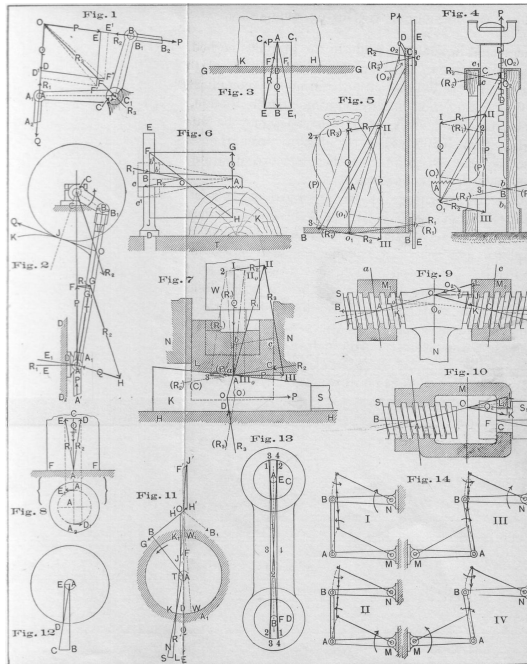


Figure 8: Graphical constructions of G. Herrmann (From [30])

A noteworthy contribution is due to H. Lorenz [31] who included in his textbook the free-response solution of a mass and spring with Coulomb friction.

The influence of friction in sliding and hinge joints during the static analysis of mechanisms is also discussed more recently by B. Paul [32]. The analysis is executed under the assumption of impending motion. In his textbook is outlined a procedure strictly valid only in the limit of vanishing coefficient of friction. In particular, for the slider joints, five possible orientations of the slider within a guide with a small clearance are considered (see Figure 9). The fifth mode, although theoretically possible, is excluded from the analysis.

With reference to Figure 9, let N_1 and N_2 be the force components orthogonal to the direction of relative motion slider-guide and $F_1 = -\mu \text{sign}(v_r)N_1$, $F_2 = -\mu \text{sign}(v_r)N_2$ the corresponding friction forces. For consistency with the compressive load exerted between slider and guide, the line of action of N_1 and N_2 is expected to be within the length of the slider. Thus, the distance e of these lines of action with respect to revolute center P must satisfy the inequalities $-a' \leq e \leq a''$.

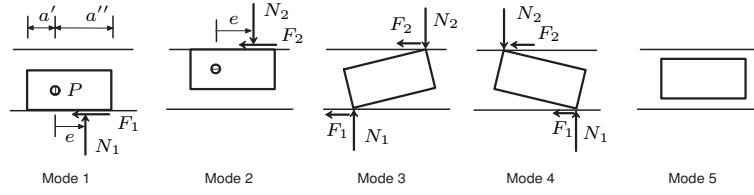


Figure 9: Possible orientations of slider and associated reactions (adapted from [32])

Assuming no friction, reactive force N_0 and torque M_0 about P are initially computed, then according to the prevailing contact mode, the appropriate set of formulas is applied:

- Contact mode 1

$$N_1 = N_0, \quad e = \frac{M_0}{N_0}, \quad (20)$$

- Contact mode 2

$$N_2 = -N_0, \quad e = \frac{M_0}{N_0}, \quad (21)$$

- Contact mode 3

$$N_1 = \frac{a''N_0 - M_0}{a' + a''}, \quad N_2 = -\frac{a'N_0 + M_0}{a' + a''}, \quad (22)$$

- Contact mode 4

$$N_1 = \frac{a''N_0 + M_0}{a' + a''}, \quad N_2 = -\frac{a'N_0 - M_0}{a' + a''}. \quad (23)$$

- Contact mode 5 (unlikely to occur and of little interest in problems of Statics).

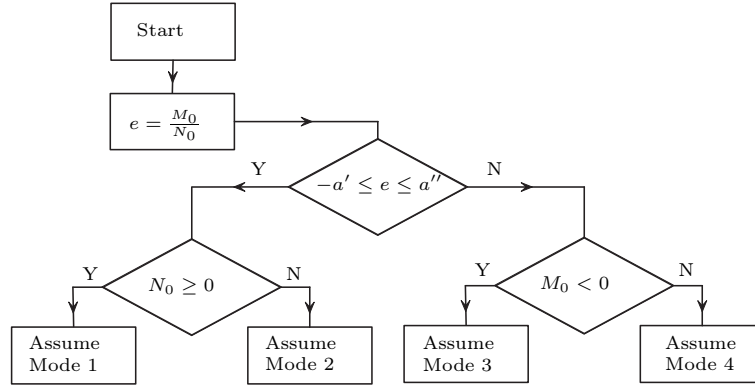


Figure 10: Logic to establish contact mode between slider and guide (adapted from [32])

The contact mode is *a priori* unknown, but it is determined following the logic summarized in the flow-chart of Figure 10. According to B. Paul, the computed mode should be correct for the practical values of μ used in machine dynamics simulation.

Once the prevailing mode is provisionally established, the contact forces N_1 and N_2 are recalculated in the presence of friction. If these are negative, then a different contact mode should be assumed.

The method described by A.S. Hall [33], aimed to inverse dynamic analysis, can be summarized in the following steps:

1. Write all forces and moment equations, including the appropriate friction terms.
2. Set all friction terms equal to zero and solve for the forces.
3. Use the results of step 2 to evaluate the friction terms, substitute into the equations and solve again.
4. Re-evaluate the friction terms based on the results of step 3 and repeat until a satisfactory accuracy is obtained.

The case of indeterminacy of friction force due to stiction is not contemplated, but the possible force situations in a straight slider joint are considered (see Figure 11) in the case of a small clearance.

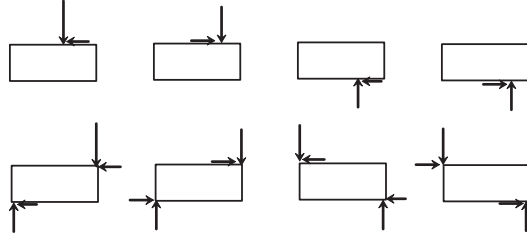


Figure 11: Possible force situations in a straight slider kinematic pair (adapted from [33])

C. Bagi [34] deduced all equations required for the time response analysis of a four-bar linkage with pair bearings affected by Coulomb friction. Inertia effects are included, but the stiction phenomena is not taken into account. The modeling of friction forces in journal bearings is based on the use of the friction circle concept.

J. de Jalón and E. Bayo [28] discussed in their textbook the procedure originally proposed by E.J. Haug *et al.* [35].

The procedure can be summarized in the following steps:

1. When all relative velocities v_r in the kinematic pairs are different than zero, the system of equation of motion

$$\begin{bmatrix} M & \Psi_q^T \\ \Psi_q & 0 \end{bmatrix} \begin{Bmatrix} \ddot{q} \\ \lambda \end{Bmatrix} = \begin{Bmatrix} Q + Q_a(\lambda) \\ \gamma \end{Bmatrix} \quad (24)$$

is iteratively solved.

2. When the relative velocity at the r kinematic pair is zero, then a stiction constraint

$$\Psi^r = 0 \quad (25)$$

is added and the following linear system solved

$$\begin{bmatrix} M & \Psi_q^T & \Psi_q^{rT} \\ \Psi_q & 0 & 0 \\ \Psi_q^r & 0 & 0 \end{bmatrix} \begin{Bmatrix} \ddot{q} \\ \lambda \\ \lambda^r \end{Bmatrix} = \begin{Bmatrix} Q \\ \gamma \\ \gamma^r \end{Bmatrix} \quad (26)$$

3. From λ^r the tangent force F_c introduced by the stiction constraint is computed. If such a force satisfies the Coulomb inequality $F_c \leq \mu_s |N|$, then the constraint is maintained, otherwise is released.

5 Dynamic analysis of planar linkages with Coulomb friction

It is assumed that:

- the linkage satisfies the Grübler or Kutzbach criterion for the computation of the degrees-of-freedom, thus there are not redundant constraints;
- there is not stiction in the kinematic pairs.

Decomposed the mass matrix such that $[M] = [M]^{1/2} [M]^{1/2}$, the solution of the matrix equation of motion (24) is executed in two steps.

In fact, from the computational point of view it is convenient to split the computation of Lagrange multipliers from the one of accelerations.

For this purpose, (24) is rewritten as follows [36]

$$\begin{bmatrix} L & 0 \\ H^T & -L_1^T \end{bmatrix} \begin{bmatrix} L^T & H \\ 0 & L_1 \end{bmatrix} \begin{Bmatrix} \ddot{q} \\ \lambda \end{Bmatrix} = \begin{Bmatrix} Q + Q_a(\lambda) \\ \gamma \end{Bmatrix} \quad (27)$$

where

$$[L] = [M]^{1/2} , \quad (28)$$

$$[H] = [L^{-1}]^T [\Psi_q]^T , \quad (29)$$

$$[L_1] = \text{chol}([H]^T [H]) . \quad (30)$$

Thus, it can be demonstrated that

$$\{\lambda\} = [L]^{-1} \{\lambda_1\} \quad (31a)$$

with

$$\{\lambda_1\} = [L_1]^{-1} ([H]^T [L]^{-1} \{Q + Q_a(\lambda)\} - \{\gamma\}) . \quad (31b)$$

Since Q_a depends on λ , a fixed point iteration procedure must be applied for the computation of Lagrange multipliers. In most of the cases few iterations are needed for convergence. However, computational improvements can be adopted, as discussed in [37].

Since $[L_1]$ is an upper triangular matrix, the use of specialized procedures (*e.g.* DTRDI of LAPACK) is recommended for its inversion.

Afterwards, the generalized accelerations vector is computed by means of

$$\{\ddot{q}\} = [L^{-1}]^T ([L]^{-1} \{Q + Q_a\} - [H] \{\lambda\}) \quad (32)$$

or, alternatively, using the formula from the Udwadia-Kalaba formulation [38, 39, 40]

$$\{\ddot{q}\} = \{\ddot{q}_f\} + [M]^{-1/2} [D]^+ (\{\gamma\} - [\Psi_q] \{\ddot{q}_f\}) . \quad (33)$$

where

$$\{\ddot{q}_f\} = [M]^{-1} \{F\} , \quad (34)$$

$$[M]^{-1} = [M]^{-\frac{1}{2}} [M]^{-\frac{1}{2}} , \quad (35)$$

$$[D] = [\Psi_q] [M]^{-\frac{1}{2}} , \quad (36)$$

and $[D]^+$ is the $[D]$ pseudo-inverse matrix.

It is interesting to observe that the discussed dynamic formulation splits the computation of Lagrange multipliers from accelerations. In other words, fixed point iteration procedure needs only to be applied to equation (31a) and not to the (24). With the Coulomb model, as demonstrated by the Painlevé paradox, the existence and uniqueness of a solution could not be guaranteed. Definitive statements on the existence of the solution cannot be made observing only the convergence of the fixed point iteration [37]. In fact, the divergence of the iteration is a necessary but not sufficient condition for nonexistence of solution. Moreover, if the iterative procedure does not converge one cannot conclude that the solution does not exist.

With the Dahl model, at current time t , the vectors

$$\{z\} = \{ z_1 \quad z_2 \quad \dots \quad z_J \}^T , \quad (37)$$

$$\{v_r\} = \{ v_{r_1} \quad v_{r_2} \quad \dots \quad v_{r_J} \}^T , \quad (38)$$

$$\{\sigma\} = \{ \sigma_1 \quad \sigma_2 \quad \dots \quad \sigma_J \}^T , \quad (39)$$

$$\{F_a\} = \{ \sigma_1 z_1 \quad \sigma_2 z_2 \quad \dots \quad \sigma_J z_J \}^T \quad (40)$$

are known. The fixed point iteration applied to (31a) is required for computing F_{c_k} ($k = 1, 2, \dots, J$). At the end of this iteration the vector $\{F_c\}$ of Coulomb friction forces is obtained and the procedure can pass to the integration subroutine the accelerations vector $\{\ddot{q}\}$, estimated by means of (32) or (33), and the vector

$$\{\dot{z}\} = \{v_r\} - \left\{ \begin{array}{c} \frac{F_{a_1} |v_{r_1}|}{F_{c_1}} \\ \vdots \\ \frac{F_{a_J} |v_{r_J}|}{F_{c_J}} \end{array} \right\} . \quad (41)$$

At time $t + \Delta t$ the numerical integration subroutine will reconstitute positions $\{q\}$, velocities $\{\dot{q}\}$ and the vector $\{z\}$ required by the Dahl model.

6 Modeling of friction forces in lower kinematic pairs

In the frictionless case, the generalized reaction force vector, reduced to the joint Cartesian frame, can be recovered through the following relationship

$$\left\{ {}^{i_k} Q_{r_k}^{(i)} \right\} = [R_{i_k}] \left[\begin{array}{cc} \Psi_{q_{3i-2}}^k & \Psi_{q_{3i-2}}^{k+1} \\ \Psi_{q_{3i-1}}^k & \Psi_{q_{3i-1}}^{k+1} \\ \Psi_{q_{3i}}^k & \Psi_{q_{3i}}^{k+1} \end{array} \right] \left\{ \begin{array}{c} \lambda_k \\ \lambda_{k+1} \end{array} \right\} , \quad (42)$$

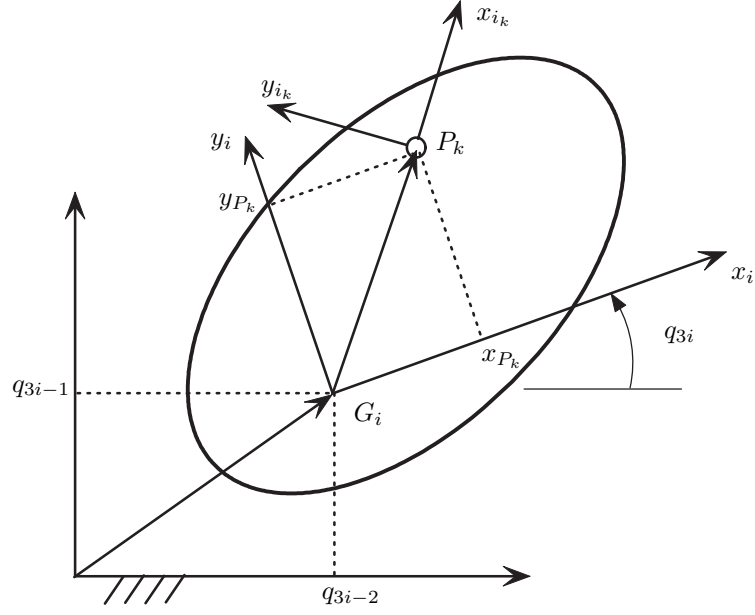


Figure 12: Cartesian system of axes: Nomenclature

where [29, 35]

$$[R_{i_k}] = \begin{bmatrix} -[C_{i_k}]^T [A_i]^T & 0 \\ \{^i s_k\}^T [V] [A_i]^T & -1 \end{bmatrix} \quad (43)$$

$$\{^i_k F\} = \{ \ ^i_k F_x \quad \ ^i_k F_y \}^T, \quad (44)$$

$$\{^i s_k\} = \{ \ x_{P_k} \quad y_{P_k} \}^T, \quad (45)$$

$$[V] = \begin{bmatrix} 0 & 1 \\ -1 & 0 \end{bmatrix}. \quad (46)$$

Due to the presence of friction, force component F_{a_k} tangential to the bearing surface will appear. Since N_k denotes the normal force, then the following equalities hold

$$F_{c_k} = \mu_d N_k, \quad (47)$$

F_{a_k} , according to Dahl model, follows from (16).

The direction of F_{a_k} is opposing the relative motion between the kinematic elements of the pair. The components of N_k are initially obtained from the Lagrange multipliers assuming absence of friction. Since the computation of Lagrange multipliers depends on the external forces, a fixed-point iteration is required for computing both N_k and F_{c_k} . For this purpose it is necessary to preliminary reduce the friction force to G_i and then transform its components in $O - XY$. In the following subsections the algebraic equations required for the computation of generalized external forces due to the presence of friction will be deduced for the case of revolute and prismatic pairs.

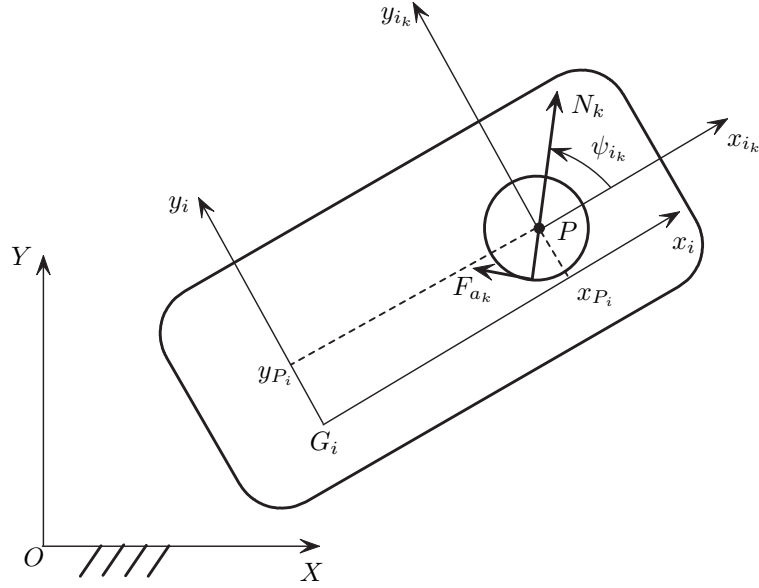


Figure 13: Friction force in a revolute pair: Nomenclature

6.1 Revolute pair

For the frictionless case, assuming $[C_{i_k}] = [I]$ and the origin P_k in the center of the revolute pair, from equation (42) one obtains

$$\{N_k\} = \begin{Bmatrix} {}^{i_k}F_x \\ {}^{i_k}F_y \end{Bmatrix} = - \begin{Bmatrix} \lambda_k \cos q_{3i} + \lambda_{k+1} \sin q_{3i} \\ -\lambda_k \sin q_{3i} + \lambda_{k+1} \cos q_{3i} \end{Bmatrix}. \quad (48)$$

The presence of Dahl friction generates the tangential force

$$\{F_{a_k}\} = \begin{cases} \begin{Bmatrix} -F_{a_k} \sin \psi_{i_k} \\ F_{a_k} \cos \psi_{i_k} \end{Bmatrix} & (\dot{q}_{3i} - \dot{q}_{3j}) < 0 \\ \begin{Bmatrix} F_{a_k} \sin \psi_{i_k} \\ -F_{a_k} \cos \psi_{i_k} \end{Bmatrix} & (\dot{q}_{3i} - \dot{q}_{3j}) > 0 \end{cases} \quad (49)$$

where

$$\psi_{i_k} = \text{ATAN2} \left({}^{i_k}F_y, {}^{i_k}F_x \right). \quad (50)$$

Hence, the corresponding generalized external force on the i^{th} body is

$$\{Q_{a_k}^{(i)}\} = \begin{Bmatrix} [A_i] \{F_{a_k}\} \\ \{{}^i t_k\}^T [B_i]^T [A_i] \{F_{a_k}\} \end{Bmatrix}, \quad (51)$$

where

$$\{{}^i t_k\} = \begin{Bmatrix} x_{P_i} \\ y_{P_i} \end{Bmatrix} + \begin{Bmatrix} r_k \cos(\pi + \psi_{i_k}) \\ r_k \sin(\pi + \psi_{i_k}) \end{Bmatrix}. \quad (52)$$

Analogous computations need to be executed for $\{Q_{a_k}^{(j)}\}$. The value of relative velocity is $v_{r_k} = (\dot{q}_{3i} - \dot{q}_{3j})r$, where r is the radius of the pin.

The proposed modeling is somewhat different from the one described in [35]. In such a reference only the torque generated by the tangential friction force component F_{a_k} is considered. This approximation is valid only for low values of μ_d .

6.2 Prismatic pair

For the frictionless case, the generalized reaction force due to a prismatic pair has two non zero components:

- a force ${}^i F_y$ normal to the axis of the pair;
- a torque τ_z

These components can be expressed as a function of Lagrange multipliers by means of (42).

With reference to the geometry of Figure 14, the joint system of axes has the origin in the corner $P_k \equiv B_i$ of the slider. The kinematic constraints for the prismatic pair follow requiring that:

- the point C_j of body j belong to the line, parallel to the axis slider, through the corners A_i, B_i of slider i ;
- there is not any relative rotation between the two bodies i and j connected by the pair.

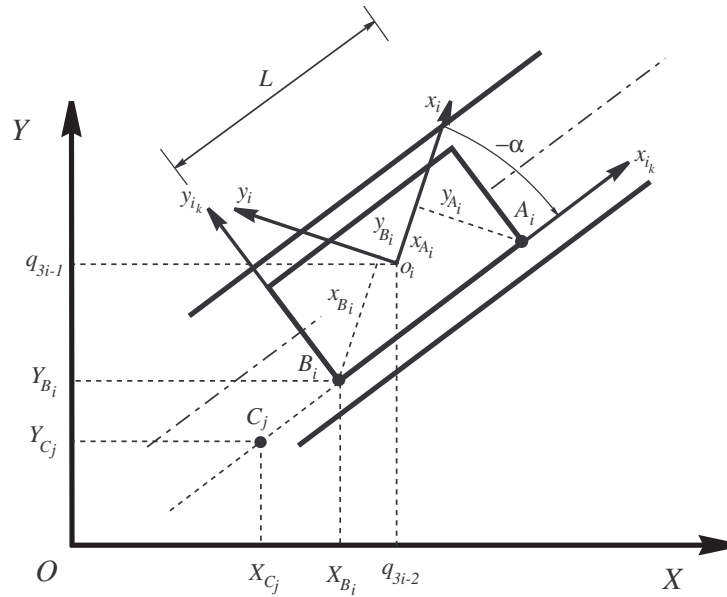


Figure 14: Joint system of axes in a prismatic pair

From (42) follows

$$\begin{Bmatrix} {}^i_k F_x \\ {}^i_k F_y \\ \tau_z \end{Bmatrix} = \begin{Bmatrix} K_1 \\ K_2 \\ K_3 \end{Bmatrix}, \quad (53)$$

where

$$\begin{aligned} K_1 &= 0, \\ K_2 &= \lambda_k [(Y_{B_i} - Y_{A_i}) \sin(q_{3i} + \alpha) - (X_{B_i} - X_{A_i}) \cos(q_{3i} + \alpha)], \\ K_3 &= \lambda_k [(q_{3i-1} - Y_{B_i})(Y_{B_i} - Y_{A_i}) \\ &\quad + (X_{B_i} - q_{3i-2})(X_{A_i} - X_{B_i}) - H_1] - \lambda_{k+1}. \end{aligned}$$

Due to friction, a force components F_{c1} and F_{c2} along the prismatic pair axis appear. These forces are always opposite to relative velocity between kinematic elements.

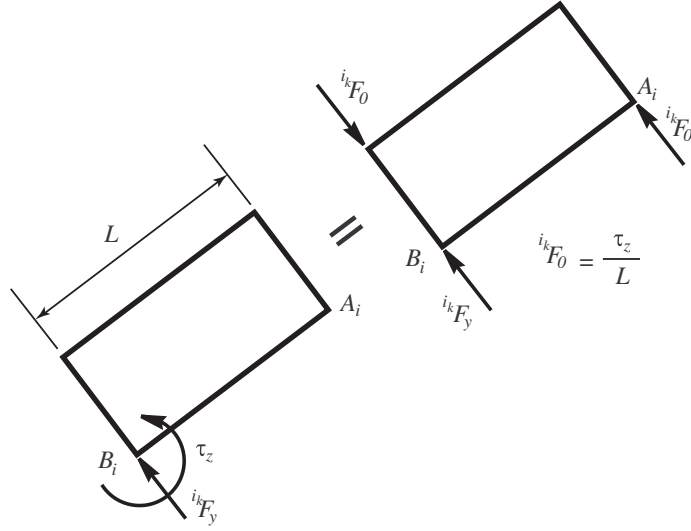


Figure 15: Equivalent system of forces

With reference to Figure 15, let us consider an equivalent system of forces. The torque τ_z is substituted by two forces

$${}^i_k F_0 = \frac{\tau_z}{L} \quad (54)$$

of equal magnitude, but different direction, acting on the opposite corners of the slider.

Hence, on the slider will be acting the following normal force components

$$\begin{aligned} N_1 &= {}^i_k F_y - {}^i_k F_0, \\ N_2 &= {}^i_k F_0. \end{aligned}$$

The resultant Coulomb friction force, when relative velocity $v_{ij} \neq 0$, is

$$F_c = F_{c1} + F_{c2} = -\text{sgn}(v_{ij}) \mu_d (N_1 + N_2). \quad (55)$$

The relative velocity between the kinematic elements can be obtained by means of the following expression

$$v_{ij} = \left\{ \begin{array}{c} \dot{X}_{A_i} - \dot{X}_{C_j} \\ \dot{Y}_{A_i} - \dot{Y}_{C_j} \end{array} \right\}^T \{u\} , \quad (56)$$

with

$$\{u\} = \text{vers} \left\{ \begin{array}{c} X_{A_i} - X_{B_i} \\ Y_{A_i} - Y_{B_i} \end{array} \right\} , \quad (57)$$

where *vers* means the unit vector.

Finally, after introducing the local coordinates of corners *A* and *B* in local system of axes

$$\left\{ {}^i b_k \right\} = \left\{ \begin{array}{c} x_{B_i} \\ y_{B_i} \end{array} \right\} , \quad (58)$$

the generalized friction forces acting on bodies *i* and *j* are respectively expressed by the following equations:

$$\left\{ Q_{a_k}^{(i)} \right\} = \left\{ \begin{array}{c} [A_{i_k}] \left\{ \begin{array}{c} F_a \\ 0 \end{array} \right\}^T \\ \left\{ {}^i b_k \right\}^T [B_{i_k}]^T [A_{i_k}]^T \left\{ \begin{array}{c} F_a \\ 0 \end{array} \right\}^T \end{array} \right\} \quad (59)$$

Analogous computations need to be executed for $\left\{ Q_{a_k}^{(j)} \right\}$.

7 Numerical examples

In this section will be presented the results of numerical simulations based on the proposed approach. For this purpose a multibody dynamics code using the Matlab programming environment has been developed. The ODE routine used for numerical integration is `ode23` with the following error control parameters `RelTol=10-4` and `AbsTol=10-4`. The kinematic constraints have been modeled by means of the method described in multibody textbooks [41, 42]. In all simulations Baumgarte stabilization has not been applied. The value of parameter α is set equal to unity. The units are in the SI system.

I) Free vibration response of a single d.o.f. mass subjected to Coulomb friction

The system analyzed is depicted in Figure 16. The physical parameters of the system are as follows: Mass $m = 1$ kg, stiffness $k = 100$ N/m, $\mu=0.5$. The initial conditions are $x = 1$ m and $\dot{x} = 0$.

Since an analytical solution is available [31], this has been used as a validation test. This analytical solution has been reported in the Appendix. For comparison the displacement and acceleration plots obtained using such solution are shown in Figure 17.

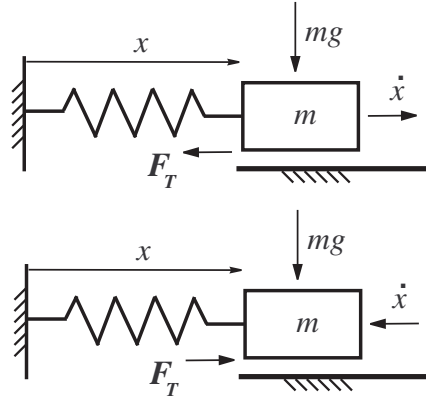


Figure 16: One d.o.f. mass-spring system subjected to Coulomb friction

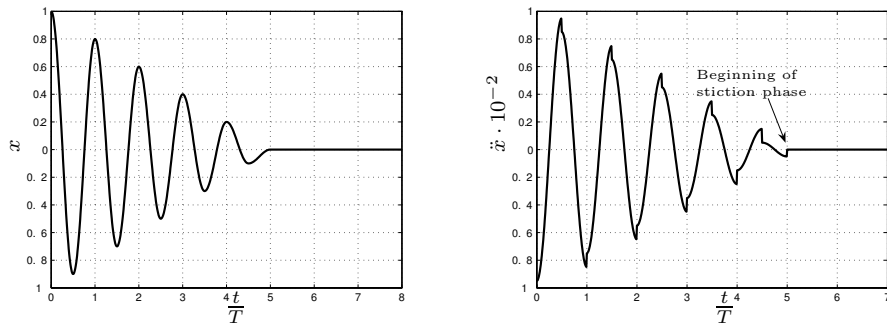


Figure 17: Analytical solution: Free response analysis of spring-mass system

In Dahl formula (17) is set $\sigma = 10000$. The authors could not find a table relating the Coulomb friction coefficients with Dahl friction parameters σ and α . The value of $\sigma = 10000$ has been chosen mainly to match as faithfully as possible the dynamic response computed analytically. (see Figure 17). As stated before, σ and α parameters should be identified through experiments.

The plots of mass position, velocity and acceleration are shown in Figure 18.

The simulation has been carried out also using the Coulomb model. The response plots of displacements and velocities are essentially identical with those obtained with the Dahl model. For this reason they will be not herein reproduced. The main difference can be observed in the acceleration plot during the stiction phase. The plot of Figure 20 shows the friction force computed with the Dahl model. After the the beginning of the stiction phase the friction force continues to oscillate due to the elastic component of the Dahl force which is never damped out.

Table 1 summarizes the computational effort data required for numerical integration of the equations of motion using the classical Coulomb and Dahl models. These data have been recorded from the Matlab output.

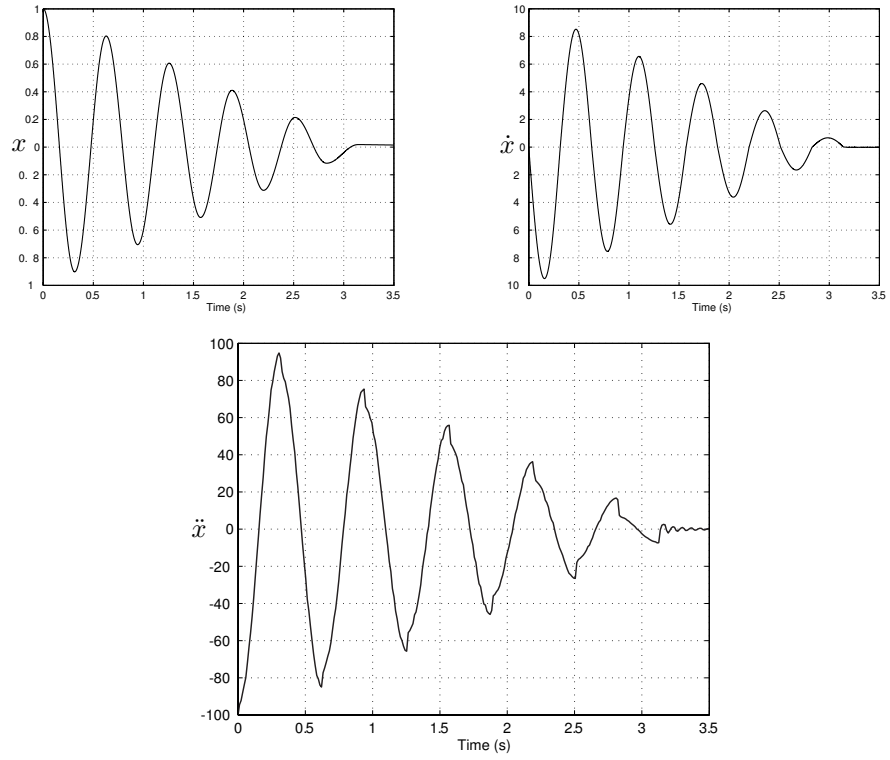


Figure 18: Dahl model: Free vibration response analysis (position, velocity and acceleration) of spring-mass system

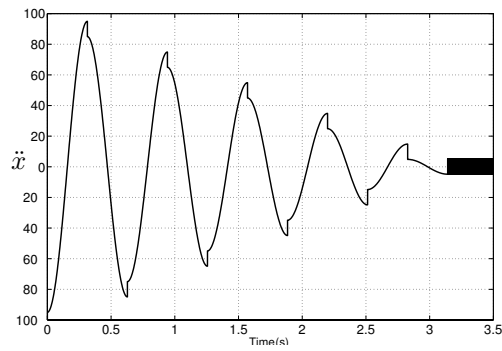


Figure 19: Coulomb model: Free vibration response analysis (acceleration) of spring-mass system

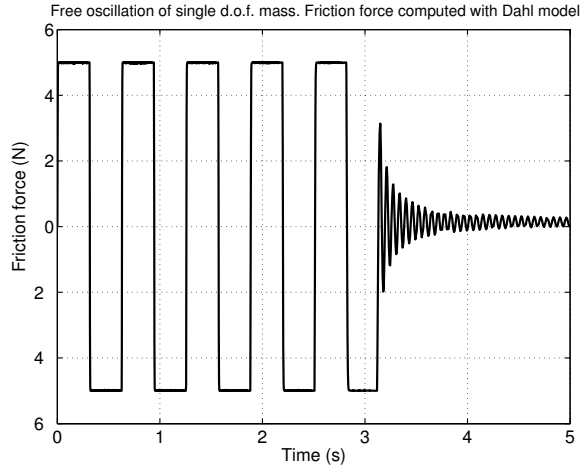


Figure 20: Friction force computed with the Dahl model

Table 1: Free vibration response of mass-spring system: Comparison of computational efficiency of Coulomb and Dahl friction models.

Friction model	Successful steps	Failed attempts	Functions evaluations
Coulomb	3581	501	12247
Dahl	8371	155	25579

II) Free vibration response of a two d.o.f. mass-pendulum system subjected to Coulomb friction

The second system analyzed is a two d.o.f. mass-pendulum system shown in Figure 21.

The physical parameters of the system are as follows: Slider mass $m_1 = 1$ kg, bar pendulum mass and moment of inertia $m_2 = 1$ kg, $I_2 = 0.1$ kgm². The bar has length $L = 1$ m and the center of mass is in the middle. The mass is uniformly distributed along the bar. The friction coefficient in the prismatic and revolute pairs is $\mu = 0.1$. The pin radius is $r = 0.3$ m. The initial conditions are $x = \theta = 0$, $\dot{x} = \dot{\theta} = 0$. The plots of mass position x and velocity \dot{x} and bar angular position θ and angular velocity $\dot{\theta}$ are reported in the Figures 22 and 23, respectively. In order to appreciate the influence of the σ parameter on numerical results, the Dahl model has been initially used with $\sigma = 10$ and then with $\sigma = 300$ (see Figure 24).

With $\sigma = 300$ a faster decay of the vibration is observed. This result is consistent with the physical significance of σ discussed in the section 3 dedicated to the description of Dahl model.

The numerical results for positions and velocities of the first example appear consistent with those obtained analytically. The plot of accelerations differ mainly in the

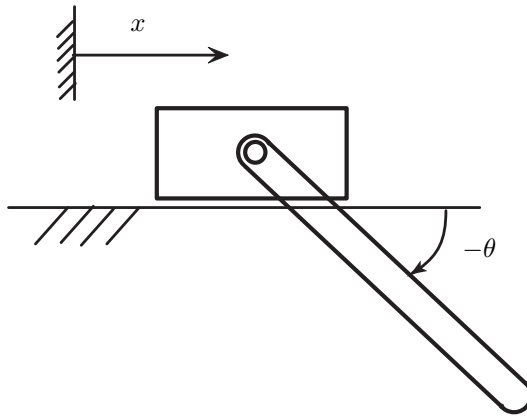


Figure 21: Two d.o.f. mass-pendulum system subjected to Coulomb friction

last part.

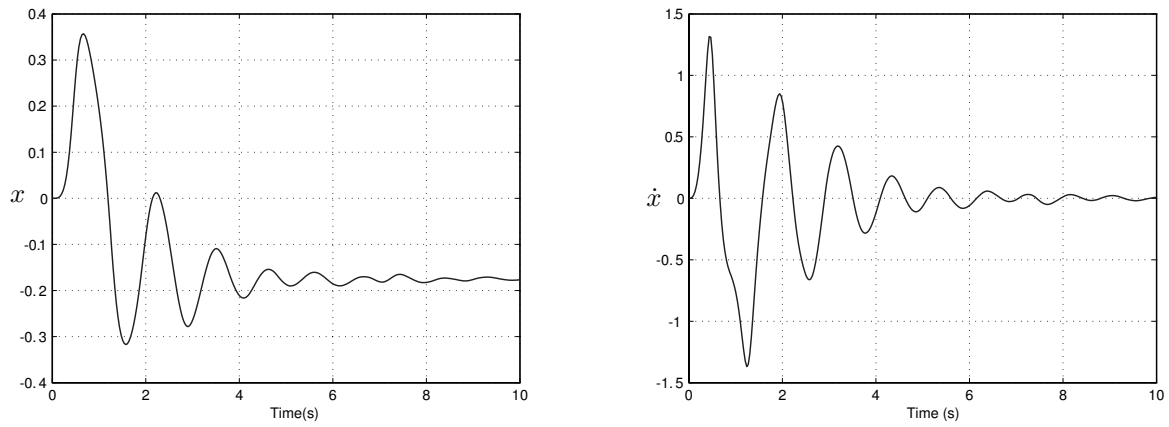


Figure 22: System response of the two d.o.f. mass-pendulum system: mass position and velocity ($\sigma = 10$)

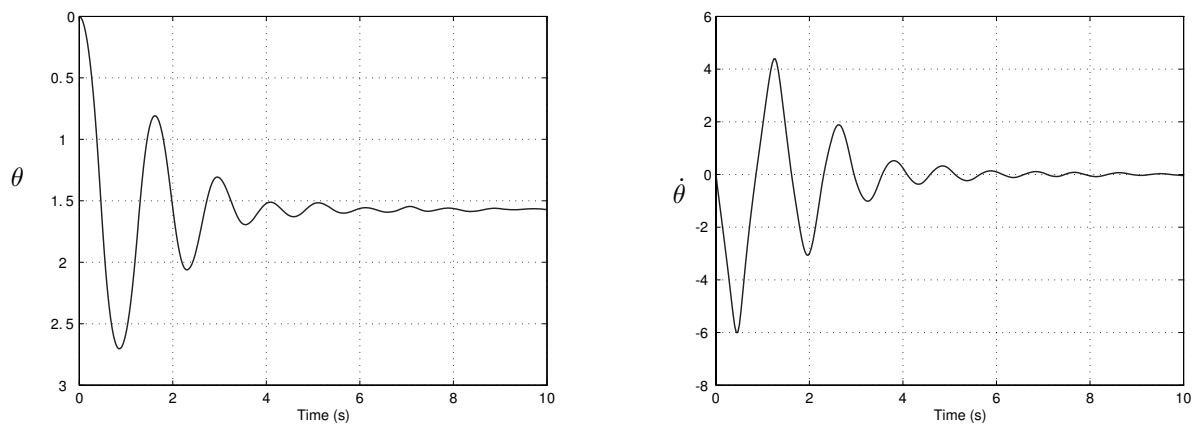


Figure 23: System response of the two d.o.f. mass-pendulum system: bar angular position and velocity ($\sigma = 10$)

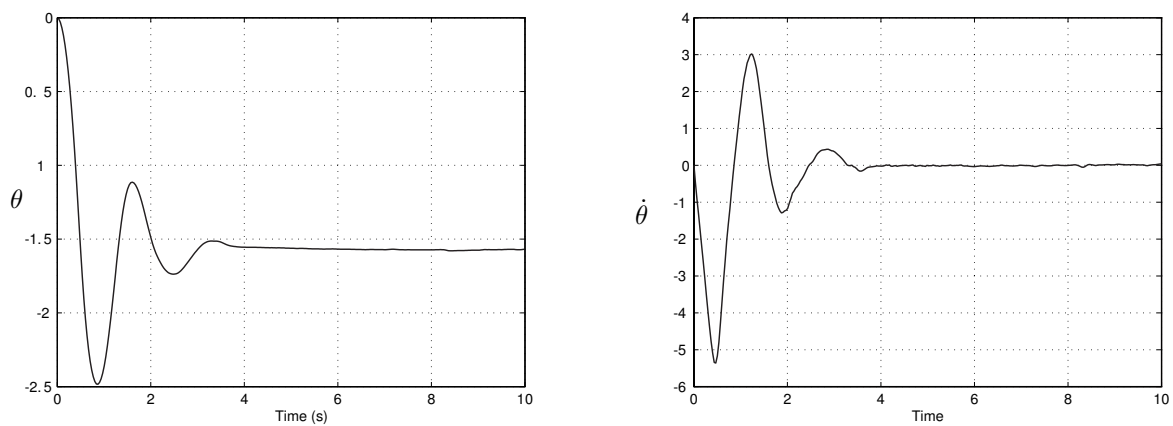


Figure 24: System response of the two d.o.f. mass-pendulum system: bar angular position and velocity ($\sigma = 300$)

8 Conclusions

This paper discussed the following items:

- introduction of the Dahl friction model in a multibody dynamics formulation with the purpose to overcome some of the difficulties associated with the Coulomb dry friction model;
- the modeling of friction forces in lower pairs;

- the computation of Lagrange multipliers in the presence of friction.

In the classic dry Coulomb model, the friction coefficients, function mainly of the materials in contact, are usually reported in standard engineering handbooks. Dahl model is more sophisticated and before using it the values of α and σ need to be experimentally identified or obtained from previous studies. Experimental procedures for σ and α identification are available in the thematic literature.

The authors' opinion is that in the field of multibody dynamics more dynamic formulations with embedded dynamic friction models should be devised. In fact, although they require the identification of parameters, usually not generally available in handbooks, there is a general consensus that these models provide a more accurate description of the physical contact behavior than the Coulomb dry friction model. Some of the mathematical disadvantages caused by the discontinuity associated with Coulomb model are avoided with the Dahl model. In fact, when $\alpha \geq 1$, the Picard-Lindelöf theorem guarantees the existence and uniqueness of the solution for the differential equation used to compute the friction force with the Dahl model. Moreover, the software implementation of the Dahl friction model is not difficult.

The discussed modeling of friction forces in lower pairs is somewhat similar to the one proposed by E.J. Haug and his coworkers. In their work only the torque generated by the tangential friction force is included in the vector of generalized forces.

Finally, it has been shown how the computation of Lagrange multipliers by means of fixed-point iteration is independent from the computation of accelerations. Because of the reduced order of matrices involved, this results into a computational gain.

References

- [1] Glocker, C.: Set-Valued Force Laws: Dynamics of Non Smooth Systems (Lectures Notes in Applied and Computational Mechanics). Springer Verlag, Berlin Heidelberg New York (2001)
- [2] Pfeiffer, F., Glocker, C.: Multibody Dynamics with Unilateral Contacts. John Wiley & Sons, (1996)
- [3] Yu Wang, Mason, M.T., Two-Dimensional Rigid-Body Collisions With Friction. ASME Journal of Applied Mechanics 59 635-642 (1992)
- [4] Han, I., Gilmore, B.J., Multi-Body Impact Motion with friction-Analysis, Simulation and Experimental Validation, *ASME Journal of Mechanical Design*, vol.115, 1993, pp.412-422
- [5] Ahmed, S., Lankarani, H.M., Pereira, M.F.O.S.: Frictional Impact Analysis in Open-Loop Multibody Mechanical Systems. ASME Journal of Mechanical Design 121, 119-127 (1999)
- [6] Lankarani, H.M., A Poisson-Based Formulation for Frictional Impact Analysis of Multibody Mechanical Systems With Open or Closed Kinematic Chains, *ASME Journal of Mechanical Design*, vol.122, 2000, pp.489-497
- [7] Stronge, W.J., Multi-body impact with friction, in *Multi-body Dynamics: Monitoring and Simulation Techniques - II*, Ed. Rahnejat, H, Ebrahimi, M., Whalley, R., Professional Engineering Publishing, 15-26 (2000)
- [8] Centea, D., Rahnejat, H., Menday, M.T., Non-linear multi-body dynamic analysis for the study of clutch torsional vibrations (judder). *Applied Mathematical Modelling* (25), 177-192 (2001)

- [9] Dahl, P.R.: Solid Friction Damping in Mechanical Vibrations. *AIAA J.* 14, 1675-1682 (1976)
- [10] Brian Armstrong-Hélouvry: *Control of Machines with Friction*. Kluwer Academic Publishers, Dordrecht (1991)
- [11] Haessig, D.A., Friedland, B.: On the modeling and simulation of friction. *ASME Journal of Dynamic Systems, Measurement, and Control* 113(3), 354-362 (1991)
- [12] Leonard, N.E., Krishnaprasad, P.S.: *Comparative Study of Friction-Compensating Control Strategies for Servomechanisms*. University of Maryland - Systems Research Center, Report TR 91-88, (1991)
- [13] Olsson, H., Åström, K.J., Canudas de Wit, C., Gäfvert, M., Lischinsky, P.: Friction Models and Friction Compensation. *European Journal of Control* 4(3), 176-195 (1998)
- [14] Song, P., Kraus, P., Kumar, V., Dupont, P.: *Analysis of Rigid Body Dynamic Models for Simulation of Systems*, Technical report, MS-CIS-00-08, University of Pennsylvania, Department of Computer Science, (2000)
- [15] Dupont, P., Hayward, V., Armstrong-Hélouvry, B., Altpeter, F.: Single State Elastoplastic Friction Models. *IEEE Transactions on Automatic Control* 47(5), 787-792, (2002)
- [16] Oh, J. *et al.*: Duhem Models for Hysteresis in Sliding and Presliding Friction, *Proceedings of the 44th Conference on Decision and Control, and the European Control Conference 2005*, Seville, Spain, December 12-15, 2005, pp. 8132-8137
- [17] Lindelöf, M.E.: Sur l'application de la méthode des approximations successives aux équations différentielles ordinaires du premier ordre. *Comptes rendus hebdomadaires des séances de l'Académie des sciences.* 114, 454-457, (1894)
- [18] Painlevé, P.: *Leçons sur le Frottement*. Cours Complémentaire de Mécanique Rationnelle, Librairie Scientifique A. Hermann, Paris (1895)
- [19] Klepp, H.J.: The existence and uniqueness of solutions for a single-degree-of-freedom system with two friction-affected sliding joints. *Journal of Sound and Vibration*, 185(2), 364-371 (1995)
- [20] Klepp, H.J.: The existence and uniqueness of solutions for the pendulum with friction. *Journal of Sound and Vibration.* 175, 138-143, (1994)
- [21] Dupont, P.E.: The Effect of Coulomb Friction on the Existence and Uniqueness of the Forward Dynamics Problem. *Proc. 1992 IEEE Int. Conf. on Robotics and Automation*, Nice, France, 1442-1447, (1992)
- [22] Painlevé, P.: Sur le lois du frottement de glissement. Different articles with the same title appered in *Comptes rendus de l'Académie des sciences*, 140, 702-707, (1905), 141, 401-405, 546-552, (1906)
- [23] Stewart, D.E.: Rigid-Body Dynamics with Friction and Impact. *SIAM Review* 42(1), 3-39, (2000)
- [24] Turner, J.D.: On the Simulation of Discontinuous Functions. *ASME Journal of Applied Mechanics* 68, 751-757 September (2001)
- [25] Threlfal D.C.: The inclusion of Coulomb Friction in Mechanisms Programs with Particular Reference to DRAM. *Mechanism and Machine Theory* 13, 475-483, (1978)

- [26] Ibrahim, R.A., <http://www.mi.uni-koeln.de/mi/Forschung/Kuepper/friction.html>
- [27] Armstrong-Hélouvry, B., Dupont, P., Canudas, C.: A survey of models, analysis tools and compensation methods for the control of machines with friction. *Automatica* 38. 1083-1138, (1994)
- [28] de Jalón, J., Bayo, E.: *Kinematic and Dynamic Simulation of Multibody Systems*. Springer Verlag, Berlin Heidelberg New York (1999)
- [29] Cheli, F., Pennestrì, E., (eds): *Kinematics and Dynamics of Multibody Systems*. Casa Editrice Ambrosiana, Milano, (2006) (*in italian*)
- [30] Herrmann, G.: *The Graphical Statics of Mechanisms*. Van Nostrand Company, New York (1900)
- [31] Lorenz, H.: *Lehrbuch der Technischen Physik: Erster Band: Technische Mechanik starrer Gebilde*. Verlag von Julius Springer, Berlin (1924)
- [32] Paul, B.: *Kinematics and Dynamics of Planar Machinery*, Prentice-Hall, (1982)
- [33] Hall, A.S.: *Notes on Mechanism Analysis*. Waveland Press Inc., (1986)
- [34] Bagci, C.: *Gross Motion Time Response Analysis of the Four-Bar Mechanism by the Method of Components with Coulomb and Viscous Damping in Pair Bearings, Linkage Design Monographs - Final Report on NSF Gk-36624*, (1976)
- [35] Haug, E.J., Wu, S.C., Yang, S.M.: Dynamics of mechanical systems with Coulomb friction, stiction, impact and constraint addition-deletion, Part I (Theory), Part II (Planar Systems). *Mechanism and Machine Theory* 21(5), 401-416, (1986)
- [36] Eich-Soellner, E., Führer, C.: *Numerical Methods in Multibody Dynamics*. B.G. Teubner, Stuttgart, (1998)
- [37] Klepp, H.J.: Kinetic friction locking for multi-body systems with friction. *Zeitschrift für Angewandte Mathematik* 46, 693-708, (1995)
- [38] Udwadia, F.E., Kalaba, R.E.: *Analytical Dynamics - A New Approach*. Cambridge University Press, (1996)
- [39] Ara Arabyan, Fei Wu: An Improved Formulation for Constrained Mechanical Systems. *Multibody System Dynamics* 2, 49-69, (1998)
- [40] de Falco, D., Pennestrì, E., Vita, L., The Udwadia-Kalaba Formulation: A Report on its Numerical Efficiency in Multibody Dynamics Simulations and on its Teaching Effectiveness. *Multibody Dynamics 2005 - ECCOMAS Thematic Conference*, Madrid 21-24 June 2005
- [41] Haug, E.: *Computer-Aided Kinematics and Dynamics of Mechanical Systems*, Allyn and Bacon (1989)
- [42] Nikravesh, P.: *Computer-Aided Analysis of Mechanical Systems*. Prentice-Hall (1988)
- [43] Lenoir, Y.: Identification des modèles tribologique par pendule. *C.R. Academie des Sciences, Paris*, t.327, Série IIb, 1259-1264, (1999)
- [44] Kermani, M.R., Pate, R.V.: Friction Identification in Robotic Manipulators, Case Studies. *Proceedings of the 2005 IEEE Conference on Control Applications*, Toronto, Canada, August 2005
- [45] Wang, Y.P, Liao, W.H., Lee, C.L., A State Approach for Dynamic Analysis of Sliding Structures, *Earthquake Engineering Structure Dynamics*, 23, 790-801, (2001)

Appendix: Free vibration response of a single d.o.f. spring-mass system subjected to Coulomb friction

Since an analytical solution is available, this case is discussed mainly for comparative purposes.

With reference to the scheme of Figure 16, let us denote with:

- m : the mass;
- k : spring stiffness;
- μ : the friction coefficient (no distinction is made between static and dynamic friction values);
- g : the acceleration gravity (set equal to 10 m/s²);
- x_0 : the position of the mass at time $t = 0$;
- T : period of free mass oscillation in the absence of friction;
- $\omega = \frac{2\pi}{T}$;
- t/T : normalized time.

Assuming zero initial velocity, until $j \leq \frac{x_0\omega^2}{2\mu g}$, the free response is described by the following function [45]

$$x\left(\frac{t}{T}\right) = x_0 \left[1 - (2j - 1) \frac{\mu g}{x_0\omega^2} \right] \cos \omega t - (-1)^j \frac{\mu g}{x_0\omega^2}, \quad \frac{j-1}{2} \leq \frac{t}{T} \leq \frac{j}{2} \quad (60)$$

The mass oscillation stops when $j > \frac{x_0\omega^2}{2\mu g}$. With the same numerical data of the example, Figure 17 shows position and acceleration of the mass computed analytically.